

This is an accepted manuscript of an article published by Taylor & available at
<https://www.tandfonline.com/doi/full/10.1080/01969722.2016.1187031>

González-Fierro, M., Monje, C.A., Balaguer, C. (2016). Fractional Control of a Humanoid Robot Reduced Model with Model Disturbances, *Cybernetics and Systems*, 47(6), pp.: 445-459.

DOI: <https://doi.org/10.1080/01969722.2016.1187031>

It is deposited under the terms of the Creative Commons Attribution-NonCommercial-NoDerivatives License (<http://creativecommons.org/licenses/by-nc-nd/4.0/>) which permits non-commercial re-use, distribution, and reproduction in any medium, provided the original work is properly cited, and is not altered, transformed, or built upon in any way.

FRACTIONAL CONTROL OF A HUMANOID ROBOT REDUCED MODEL WITH MODEL DISTURBANCES

(Short version of the title: Fractional Control of a Humanoid Robot)

M. GONZÁLEZ-FIERRO, C.A. MONJE, C. BALAGUER

System Engineering and Automation Department, University Carlos III of Madrid,

Avenida Universidad 30, 28911 Leganés, Madrid, Spain

{mgpalaci, cmonje, balaguer}@ing.uc3.es

There is an open discussion between those who defend mass distributed models for humanoid robots and those in favor of simple concentrated models. Even though each of them has its advantages and disadvantages, little research has been conducted analyzing the control performance due to the mismatch between the model and the real robot, and how the simplifications affect the controller's output. In this paper we address this problem by combining a reduced model of the humanoid robot, which has an easier mathematical formulation and implementation, with a fractional order controller, which is robust to changes in the model parameters. This controller is a generalization of the well-known PID structure obtained from the application of Fractional Calculus to control, as will be discussed in the paper. This control strategy guarantees the robustness of the system, minimizing the effects from the assumption that the robot has a simple mass distribution. The humanoid robot is modeled and identified as a triple inverted pendulum and, using a gain scheduling strategy, the performances of a classical PID controller and a fractional order PID controller are compared, tuning the controller parameters with a genetic algorithm.

Keywords: Humanoid robot model; Fractional order control; Reduced dynamic model.

I. INTRODUCTION

In recent years there has been a strong discussion between researchers in favor of using mass distributed models to model a humanoid robot, where the mass and inertia of every link are known, and those who prefer to use a simplified or concentrated mass model, where all robot dynamics are simplified and concentrated in the center of gravity, as stated in Arbulú, 2009.

Those who prefer complete dynamic models defend that they allow the representation of more complex behaviors, ensuring the accuracy of the model and reducing the complexity of the control method. Khatib et al., 2008 performed a whole-body motion hierarchically dividing the control into tasks. Arbulu et al., 2010 used Lie algebra to obtain the humanoid whole-body dynamics and reduce the computation time. Kajita et al., 2003 presented a work where the humanoid motion is accomplished controlling the momentum of a complete body model.

Many researchers make use of reduced dynamic models to control humanoids, some examples are the 2D and 3D linear inverted pendulum modes (LIPM) in Kajita et al., 1991 and Kajita et al., 2001, the cart-table presented in Kajita et al., 2003 or the angular momentum pendulum model presented in Komura et al., 2005.

The reduced models do not cover all the dynamic behavior and non linearities of the real model; however, they are commonly used and many researchers have obtained good experimental results. Kaynov et al., 2009 modeled a humanoid robot as a double inverted pendulum to study stability; Mistry et al., 2010 modeled a humanoid as an inverted pendulum of five links and performed a stand up task; Pan et al., 2004 used an evolutionary approach to control a triple inverted pendulum. Other examples of triple pendulum control are the works by Tsachouridis, 1999 with H_∞ and Xiaofeng et al., 2009 with fuzzy methods.

On the other hand, fractional calculus can be defined as a natural extension of the classical mathematics. Since the earliest theoretical contributions on fractional derivatives and integrals made by Euler, Liouville and Abel, fractional order control has drawn the attention of many researchers (Monje et al., 2010).

For convenience, Laplace domain notion is commonly used to describe the fractional integro-differential operation. The Laplace transform of the fractional derivative/integral under zero initial conditions for order α ($0 < \alpha < 1$) is given by

$$\mathcal{L}\{D_t^{\pm\alpha} f(t)\} = s^{\pm\alpha} F(s). \quad (1)$$

Podlubny et al., 1997 proposed a generalization of the classical PI and PID controllers defined as PI^λ and $PI^\lambda D^\mu$, where the integrator order λ and the differentiator order μ assume real non-integer values. He also

proved that these types of fractional order controllers have better control performances (Podlubny, 1999(a) and Podlubny, 1999(b)).

This new type of controllers encouraged a lot of works dedicated to fractional order control systems. Consequently, a considerable attention has been attracted to PI^λ , PD^μ and $PI^\lambda D^\mu$ controllers, as reviewed by Monje et al., 2010. Thereafter, numerous tuning methods have been developed for the setting of the parameters of these fractional order controllers. In Buslowicz, 2008 a numerical algorithm is proposed for checking the stability of linear continuous-time fractional order systems with delays of the retarded type. A frequency approach for the auto-tuning of fractional order $PI^\lambda D^\mu$ is proposed in Monje et al., 2008, where PI^λ is used to cancel the slope of the curve phase of a position servo system with a time delay around a frequency point and the PD^μ controller is designed to fulfill the specification of gain crossover frequency. A new stabilizing problem is presented in Caponetto et al., 2010 using a generalization of the Hermite-Biehler theorem applicable to the fractional quasi-polynomials.

Fractional calculus also extends to other kinds of control strategies different from *PID* ones, but in the case study presented in this paper we propose the use of the fractional order $PI^\lambda D^\mu$ controller as a robust alternative for the control of a humanoid robot simplified model based on the triple inverted pendulum, improving the system performance and overtaking the mismatches produced between the simplified and real models of the robot.

To test the robustness of the control system, we will compare the performances of a classical *PID* controller and the fractional order *PID* controller when the humanoid performs a standing up task from a chair. We will overload the system adding 1 Kg to every pendulum link, with the objective of evaluating the robot performance when there is a change in the mass of the model. The controller gains will be optimized using an algorithm based on differential evolution.

The rest of the paper is organized as follows. Section II presents the simplified model of the HOAP humanoid robot as a triple inverted pendulum, together with its state space representation. Section III gives some considerations on the implementation of fractional order controllers. Section IV introduces the Differential Evolution method used to tune the different controllers proposed. In Section V, the simulation results are given and discussed, concluding in Section VI with the main conclusions and future works.

II. HUMANOID ROBOT MODEL

In a very simplified way, a humanoid robot can be dynamically modeled as a triple inverted pendulum. As it can be seen in Fig. 1 (Left), we have modeled the HOAP humanoid robot as a triple pendulum, where the ankle joint of the robot corresponds to the first pendulum joint, the knee joint corresponds to the second one and the hip joint corresponds to the third one (see Fig. 1 (Right)).

The similarity is stated under the assumptions that the pendulum masses are concentrated at the tip of every link and the link masses are negligible. The control action that allows every mass m_i to move a position q_i is the torque τ_i .

Since the task we want to perform is the standing up of the robot from a chair, choosing the triple pendulum as the model allows the direct mapping between the pendulum joints and the joints needed for the robot to stand up. It is a good trade between selecting a simple inverted pendulum model and a complete model.

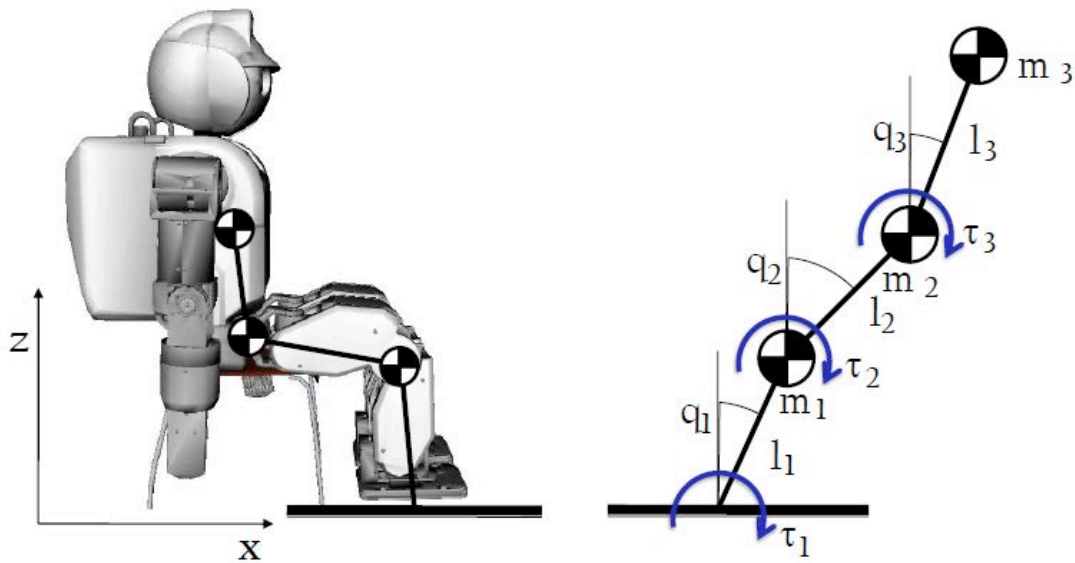


Fig. 1: Left: Reduced model of HOAP humanoid robot sitting on a chair. The proposed model is a two dimensional triple inverted pendulum with massless links and the center of mass at the tip of the pendulum. Right: Triple inverted pendulum with masses, lengths, torques and positions.

TRIPLE PENDULUM EQUATIONS

To obtain the triple pendulum equations let us define the position and velocity of every link.

$$x_1 = l_1 \sin q_1, \dot{x}_1 = l_1 \cos q_1 \dot{q}_1 \quad (2)$$

$$z_1 = l_1 \cos q_1, \dot{z}_1 = -l_1 \sin q_1 \dot{q}_1 \quad (3)$$

$$x_2 = l_1 \sin q_1 + l_2 \sin q_2 \quad (4)$$

$$\dot{x}_2 = l_1 \cos q_1 \dot{q}_1 + l_2 \cos q_2 \dot{q}_2 \quad (5)$$

$$z_2 = l_1 \cos q_1 + l_2 \cos q_2 \quad (6)$$

$$\dot{z}_2 = -l_1 \sin q_1 \dot{q}_1 - l_2 \sin q_2 \dot{q}_2 \quad (7)$$

$$x_3 = l_1 \sin q_1 + l_2 \sin q_2 + l_3 \sin q_3 \quad (8)$$

$$\dot{x}_3 = l_1 \cos q_1 \dot{q}_1 + l_2 \cos q_2 \dot{q}_2 + l_3 \cos q_3 \dot{q}_3 \quad (9)$$

$$z_3 = l_1 \cos q_1 + l_2 \cos q_2 + l_3 \cos q_3 \quad (10)$$

$$\dot{z}_3 = -l_1 \sin q_1 \dot{q}_1 - l_2 \sin q_2 \dot{q}_2 - l_3 \sin q_3 \dot{q}_3 \quad (11)$$

Articulated torques can be derived using the Lagrangian equation:

$$\frac{d}{dt} \left(\frac{\partial \mathcal{L}}{\partial \dot{q}_i} \right) - \frac{\partial \mathcal{L}}{\partial q_i} = \tau_i \quad (12)$$

where the Lagrangian is the difference between kinetic and potential energy:

$$\mathcal{L} = \mathcal{T} - \mathcal{V} \quad (13)$$

Let us define the potential energy:

$$\mathcal{V} = m_1 g z_1 + m_2 g z_2 + m_3 g z_3 \quad (14)$$

Substituting:

$$\mathcal{V} = (m_1 + m_2 + m_3) g l_1 \cos q_1 + (m_2 + m_3) g l_2 \cos q_2 + m_3 g l_3 \cos q_3 \quad (15)$$

Let us define the kinetic energy:

$$T = \frac{1}{2}m_1v_1^2 + \frac{1}{2}m_2v_2^2 + \frac{1}{2}m_3v_3^2 \quad (16)$$

where v_1 , v_2 and v_3 are the speed of the centers of mass of the inverted pendulum, $v_i^2 = \dot{x}_i^2 + \dot{z}_i^2$.

Substituting Eq. (4,...,13) into Eq. (16) and Eq. (18) and then into Eq. (15), we obtain the equation of motion of the triple pendulum, whose compact form is stated as follows:

$$v_i^2 = \dot{x}_i^2 + \dot{z}_i^2 \quad (17)$$

$$\mathbf{M} = \mathbf{H}(\mathbf{q})\ddot{\mathbf{q}} + \mathbf{C}(\mathbf{q}, \dot{\mathbf{q}})\dot{\mathbf{q}} + \mathbf{G}(\mathbf{q}) \quad (18)$$

where $\mathbf{H} \in \mathbb{R}^{3 \times 3}$ is the inertia matrix, $\mathbf{C} \in \mathbb{R}^{3 \times 3}$ is the matrix of centrifugal and coriolis forces and $\mathbf{G} \in \mathbb{R}^{3 \times 1}$ is the gravity matrix. The components of every matrix can be expressed as:

$$\begin{pmatrix} h_{11} & h_{12} & h_{13} \\ h_{21} & h_{22} & h_{23} \\ h_{31} & h_{32} & h_{33} \end{pmatrix} \begin{pmatrix} \ddot{q}_1 \\ \ddot{q}_2 \\ \ddot{q}_3 \end{pmatrix} + \begin{pmatrix} 0 & c_{12} & c_{13} \\ c_{21} & 0 & c_{23} \\ c_{31} & c_{32} & 0 \end{pmatrix} \begin{pmatrix} \dot{q}_1^2 \\ \dot{q}_2^2 \\ \dot{q}_3^2 \end{pmatrix} + \begin{pmatrix} g_1 \\ g_2 \\ g_3 \end{pmatrix} \quad (19)$$

$$h_{11} = l_1^2(m_1 + m_2 + m_3) \quad (20)$$

$$h_{22} = l_2^2(m_2 + m_3) \quad (21)$$

$$h_{33} = l_3^2 m_3 \quad (22)$$

$$h_{12} = h_{21} = (m_2 + m_3)l_1 l_2 \cos(q_1 - q_2) \quad (23)$$

$$h_{13} = h_{31} = m_3 l_1 l_3 \cos(q_1 - q_3) \quad (24)$$

$$h_{23} = h_{32} = m_3 l_2 l_3 \cos(q_2 - q_3) \quad (25)$$

$$c_{12} = -c_{21} = (m_2 + m_3)l_1 l_2 \sin(q_2 - q_1) \quad (26)$$

$$c_{13} = m_3 l_1 l_3 \sin(q_3 - q_1) \quad (27)$$

$$c_{23} = m_3 l_2 l_3 \sin(q_3 - q_2) \quad (28)$$

$$g_1 = g l_1 (m_1 + m_2 + m_3) \sin(q_1) \quad (29)$$

$$g_2 = g l_2 (m_2 + m_3) \sin(q_2) \quad (30)$$

$$g_3 = g l_3 m_3 \sin(q_3) \quad (31)$$

STATE SPACE REPRESENTATION OF THE TRIPLE PENDULUM

The inverted triple pendulum can be expressed as a dynamical system in the standard form:

$$\dot{X} = AX + BU, \quad Y = CX \quad (32)$$

where X is the state vector, U is the control vector and Y is the output vector.

To obtain the representation of the triple pendulum system let us define the following state variables:

$$X_1 = q_1, X_2 = \dot{q}_1, X_3 = q_2, X_4 = \dot{q}_2, X_5 = q_3, X_6 = \dot{q}_3.$$

Taking this into account, and reordering Eq. (20), matrices A , B and C can be obtained knowing that:

$$\dot{X}_1 = X_2, \dot{X}_3 = X_4, \dot{X}_5 = X_6 \quad (33)$$

$$\begin{pmatrix} \dot{X}_2 \\ \dot{X}_4 \\ \dot{X}_6 \end{pmatrix} = \hat{f}(X_1, X_2, X_3, X_4, X_5, X_6) \quad (34)$$

where \hat{f} contains nonlinear terms of the state variables.

To avoid the nonlinear terms, we have linearize over X_{i0} using a Taylor expansion:

$$\dot{\tilde{X}} = A \tilde{X} + B \tilde{U} \quad (35)$$

where

$$A = \left. \frac{\partial f}{\partial X} \right|_{\substack{X=X_0 \\ U=U_0}} ; \quad B = \left. \frac{\partial f}{\partial U} \right|_{\substack{X=X_0 \\ U=U_0}} \quad (36)$$

and $\tilde{X}_i = X_i - X_{i0}$.

Since the desired trajectory has a wide variation, we have selected three regions of linearization, obtaining three subsystems. We have divided the desired trajectory in three regions and we have chosen the middle point of every region as the linearization point. In Fig. 2 the selected linearization positions are shown. The result is three linear systems that are going to be controlled with standard and fractional order PID controllers using the differential evolution approach, as will be explained later.

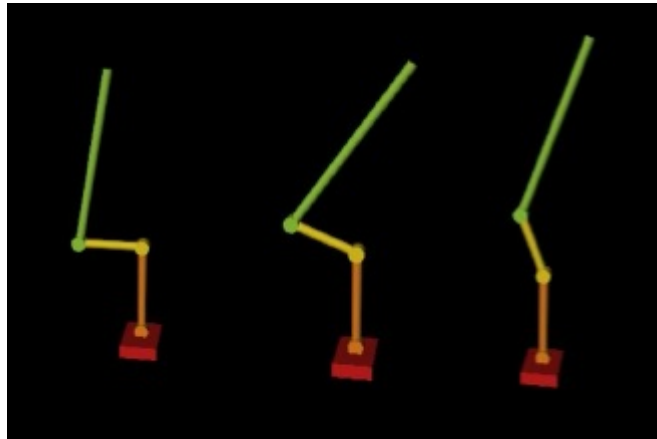


Fig 2: The three positions of the system linearization. Every position is a point of linearization and defines a linear system

III. IMPLEMENTATION OF THE FRACTIONAL ORDER CONTROLLER

Before introducing the differential evolution method used for the tuning of the different controllers proposed in this paper, some considerations on the implementation of the fractional order $PI^{\lambda}D^{\mu}$ controller have to be taken into account (Oustaloup et al., 2010 and Caponetto et al., 2010). An extensive review regarding this topic is given by Monje et al., 2010.

The generalized transfer function of this controller is given by

$$c(s) = k_p + \frac{k_i}{s'} + k_d s^\mu \quad (37)$$

In general, when fractional order controllers have to be implemented or simulations have to be performed, fractional transfer functions are usually replaced by integer transfer functions with a behavior close enough to the one desired, but much easier to handle. There are many different ways of finding such approximations but unfortunately it is not possible to say that one of them is the best, because even though some of them are better than others in regard to certain characteristics, the relative merits of each approximation depend on the differentiation order, on whether one is more interested in an accurate frequency behavior or in accurate time responses, on how large admissible transfer functions may be, and other factors like these (Monje et al., 2010).

In this work a frequency identification method performed by the Matlab function *invfreqs* has been used. With this method a rational transfer function is obtained whose frequency response fits the frequency response of the original irrational transfer function within a selected frequency range. This method is chosen due to its accuracy in the frequency range of interest, which can be adjusted by selecting the number of poles/zeros of the rational transfer function.

IV. DIFFERENTIAL EVOLUTION

Differential Evolution (DE) is a stochastic search optimization method based on genetic algorithms first proposed by Storn and Price, 1997. It is widely used in SLAM (Moreno et al., 2009), multiobjective optimization (Xue et al., 2003), pattern recognition (Bueno et al., 2012) or constraint optimization (Huang et al., 2007).

This algorithm selects a random initial population over a bounded domain x_{min} and x_{max} , generating N_p population members. Similarly to other evolutionary algorithms, it perturbs the population, generating new members that are going to be evaluated in a fitness function.

The selection and combination of new points are randomly chosen from three individuals. Two of the members, x_{r1} and x_{r2} , are subtracted and multiplied by a weight F , and then added to another x_{r3} giving a trial solution:

$$u_0 = x_{r3} + F(x_{r1}, x_{r2}) \quad (38)$$

This solution u_0 is evaluated in the fitness function and compared with the rest of the vector of the same index. This process is repeated until a population of N_p has competed against the trial solution randomly generated. Once the last vector has been evaluated, the best members are selected for the next iteration. The computation ends when a final condition has been achieved. Usual conditions are time, number of iterations or a specific value of the fitness function.

In this paper we have used differential evolution to optimize the values of the PID controller gains $k_p, k_i, k_d \in \mathbb{R}^{3 \times 3}$ and the gains and orders of the fractional order controller k_p, k_i, k_d, λ and μ .

V. RESULTS AND DISCUSSION

IDENTIFICATION OF PENDULUMS PARAMETERS

To characterize the triple inverted pendulum that models our Hoap humanoid robot a system identification is performed based on the work by Tang et al., 2008. For this purpose we have used DE optimizer, computing a triple pendulum's Zero Moment Point (ZMP) trajectory and comparing it with the real ZMP measurement of the robot feet FSR sensors (Fig. 3), minimizing the quadratic difference. The results are shown in Table 1.

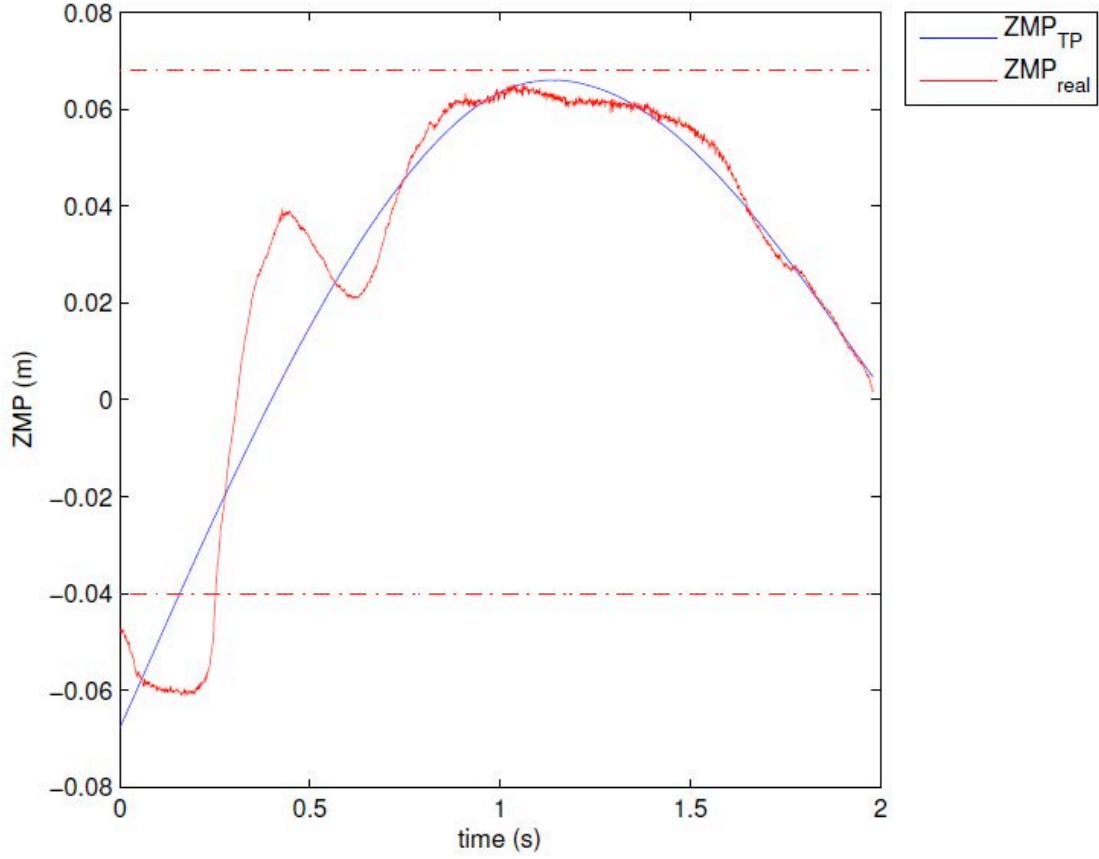


Fig. 3: ZMP trajectory of the triple inverted pendulum (ZMP_{TP}) and ZMP of the real robot (ZMP_{real}) measured with the feet sensors

The multibody ZMP equation in the sagital plane is

$$ZMP = \frac{\sum_{i=1}^n m_i x_i (\ddot{z}_i + g) + \sum_{i=1}^n m_i \ddot{x}_i z_i + \sum_{i=1}^n I_{iy} \ddot{\theta}_{iy}}{\sum_{i=1}^n m_i (\ddot{z}_i + g)} \quad (39)$$

The reason why we use the ZMP to perform the identification is because ZMP is a measurement of stability, and we can obtain a real ZMP directly from robot sensors. This is more intuitive and gives more information than simple joint trajectories.

Table 1: Triple pendulum identification parameters

	Mass (Kg)	Link (m)
Link 1	0.505	0.167
Link 2	0.500	0.260
Link 3	3.900	0.264

Taking these parameters into account and the three operating points previously stated (Fig. 2), we obtain three linearized subsystems using Eq. (37). Each subsystem is controlled using a standard and a fractional order PID controller, whose gains $k_p, k_i, k_d \in \mathbb{R}^{3 \times 3}$ and fractional orders λ, μ are obtained using DE. To change between systems, we use a gain scheduling strategy.

The desired trajectory has been manually defined using third order splines and it simulates a stand up trajectory. The trajectory has been divided into three regions of two seconds, each one corresponding to the three subsystems. In Fig. 4 the simulated trajectory is shown.

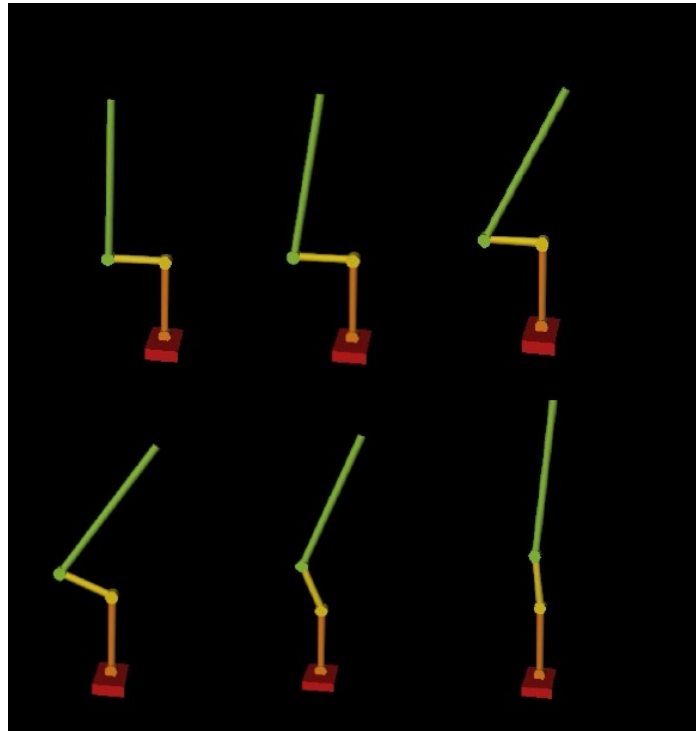


Fig. 4: Simulation of the triple inverted pendulum trajectory

Furthermore, to estimate the controller robustness, we have overloaded the pendulum masses, adding 1 Kg to each link and comparing the new responses with those obtained from the nominal system.

COMPARISON BETWEEN CLASSICAL AND FRACTIONAL ORDER CONTROLLERS

All simulations have been performed in MATLAB, using Runge-Kutta solver and a sampling time of 1 ms.

The DE algorithm produces random values of the controller gains, which are used to simulate the system in Fig. 5. The fitness function to minimize is the difference between the system output and the reference. The best member of every iteration is mutated and evaluated again until a final value of the fitness function is reached or a total number of iterations is passed. In our case, the final value is 1 and the maximum number of iterations is 50.

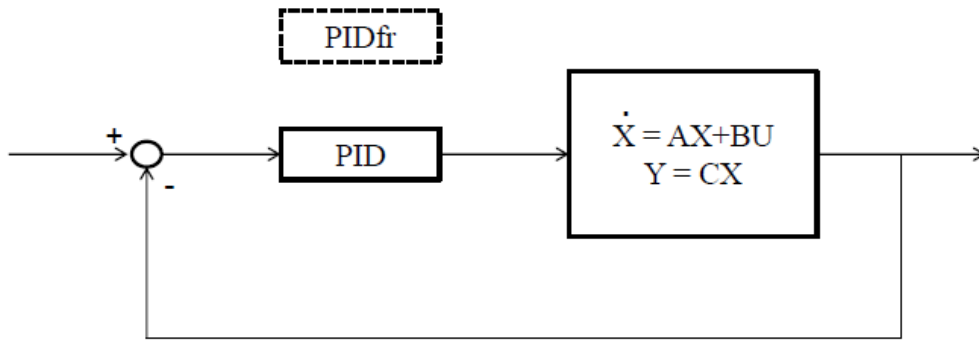


Fig. 5: Control system. The PID block is replaced by the PIDfr block when the fractional order control strategy is used

This is done for every subsystem with the standard PID gains and with the fractional order PID gains and orders.

To approximate the behavior of the fractional controller, we have used the frequency identification method *invfreqs* provided by MATLAB (Monje et al., 2010), described in Section III. The chosen crossover frequency has been 0.001 rad/s and the number of poles and zeros selected for the equivalent transfer function is 8, ensuring the fractional behavior along 4 decades of frequency. This expression is evaluated in MATLAB and implemented in the block PIDfr of Fig. 5.

For the sake of space, we are just presenting the parameters of the fractional order PID controller for the first region, similarly obtaining the corresponding controllers for the other two regions, and so for the classical PID case.

$$k_{p1} = \begin{pmatrix} 404.727 & ! 305.224 & ! 782.663 & \% \\ 1887.738 & ! 102.147 & ! 6281.782 & \downarrow \\ \# 1097.379 & ! 13.248 & 417.511 & \& \end{pmatrix}$$

$$k_{i1} = \begin{pmatrix} ! 13129.120 & 13074.195 & ! 5581.229 & \% \\ ! 1185.499 & ! 118.561 & 1321.581 & \downarrow \\ \# ! 1971.739 & ! 933.607 & 12007.290 & \& \end{pmatrix}$$

$$k_{d1} = \begin{pmatrix} 10891.500 & 6320.620 & 1687.942 & \% \\ ! 3646.421 & 1252.162 & 7721.200 & \downarrow \\ \# 1025.524 & ! 943.733 & ! 1851.324 & \& \end{pmatrix}$$

$$!_1 = 0.595, \mu_1 = ! 0.432$$

The results obtained for the three regions are presented in Fig. 6, 7 and 8, respectively.

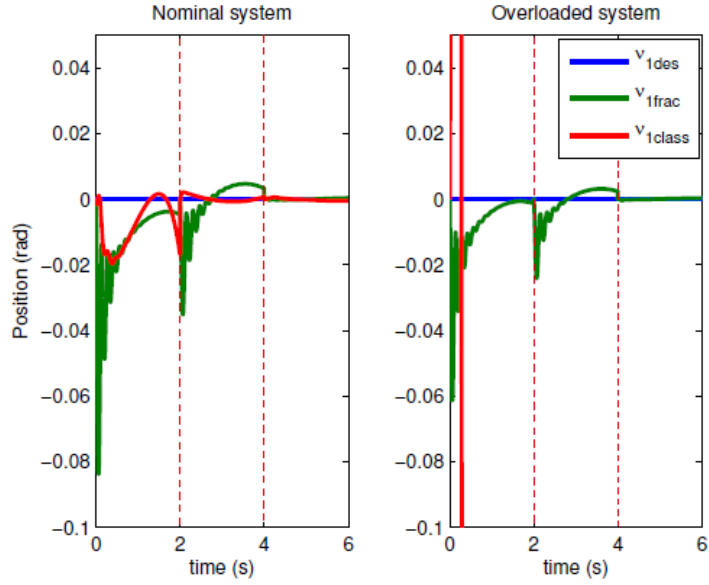


Fig. 6: System response for joint 1 for the nominal (left) and overloaded (right) subsystem. In blue is the desired trajectory, in green the trajectory with the fractional order controller and in green the trajectory with the standard PID controller. In dotted red the limits of the three linearization regions

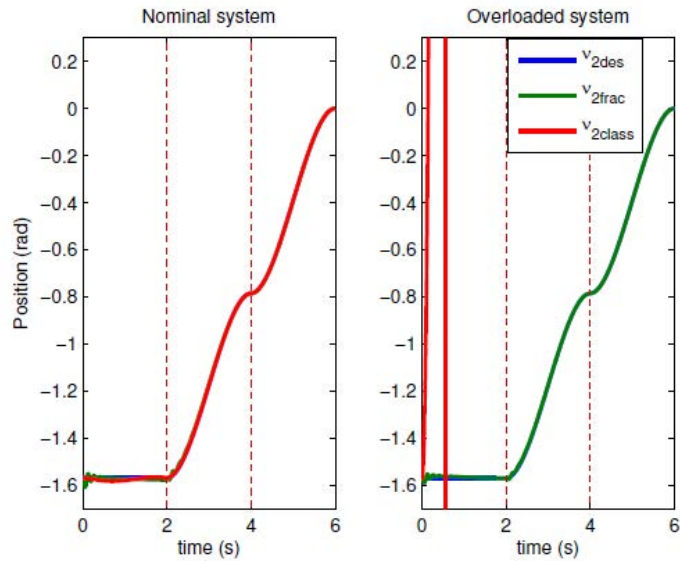


Fig. 7: System response for joint 2 for the nominal (left) and overloaded (right) subsystem. In blue is the desired trajectory, in green the trajectory with the fractional order controller and in green the trajectory with the standard PID controller. In dotted red the limits of the three linearization regions

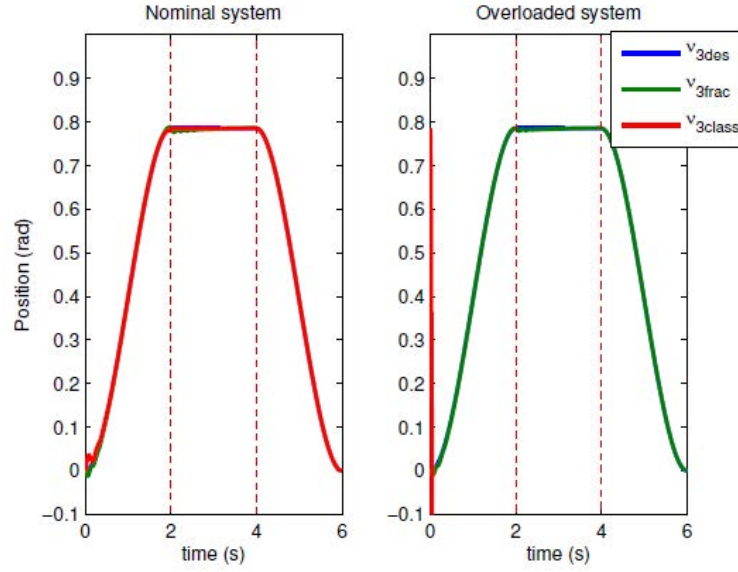


Fig. 8: System response for joint 3 for the nominal (left) and overloaded (right) subsystem. In blue is the desired trajectory, in green the trajectory with the fractional order controller and in green the trajectory with the standard PID controller. In dotted red the limits of the three linearization regions.

As can be seen, the fractional order controller keeps the stability of the system in case a significant mass mismatch appears in the model. This way, we can guarantee the robustness of the control system to uncertainties in the model, compensating this way the effects of using for simplicity a reduced model of the robot for control purposes. On the contrary, the responses with the standard PID controller are unstable for some of the joints when the system is overloaded.

VI. CONCLUSIONS AND FUTURE WORKS

This paper addresses the problem of modeling and controlling a reduced model of a humanoid robot based on the triple inverted pendulum. A control technique that uses differential evolution and a fractional order PID controller is applied, obtaining very good results.

The effect of mass mismatches between the real and the simplified model of the humanoid is compensated to a significant extent by the fractional order PID controller, which ensure the robust response of the whole system during the whole motion when a mass increase of 1 Kg is considered in each tip.

After comparing the behavior of the humanoid when performing a standing up movement using the standard PID controller and the fractional order one, it is concluded that, using differential evolution as gain optimizer, both controllers track the reference satisfactorily for the nominal case. However, when the robot is overloaded, only the fractional order controller ensures the stability of the system.

Further steps on this research will be taken towards the implementation of this control strategy in the real robotic platform.

ACKNOWLEDGEMENTS

The research leading to these results has received funding from the ARCADIA project DPI2010-21047-C02-01, funded by CICYT project grant on behalf of Spanish Ministry of Economy and Competitiveness, and from the RoboCity2030-II-CM project (S2009/DPI-1559), funded by the Research and Development Work Programme of the Community of Madrid and cofunded by Structural Funds of the EU.

REFERENCES

- Arbulu, M. 2009. Stable locomotion of humanoid robots based on mass concentrated model. *Ph.D. Thesis*, University Carlos III of Madrid.
- Arbulú, M., Balaguer, C., Monje, C., Martínez S. and Jardón, A. 2010. Aiming for multibody dynamics on stable humanoid motion with special euclidean groups. In *2010 IEEE/RSJ International Conference on Intelligent Robots and Systems (IROS'2010)*, pages 691–697.
- Bueno, J.G., Fierro, M.G., Moreno, L. and Balaguer, C. 2012. Facial gesture recognition using active appearance models based on neural evolution. In *2012 International Conference on Human-Robot Interaction (HRI'2012)*.
- Buslowicz, M. 2008. Stability of linear continuous-time fractional order systems with delays of the retarded type. *Bulletin of the Polish Academy of Technical Sciences*, 56(4).
- Caponetto, R., Dongola, G., Fortuna, L. and Gallo, A. 2010. New results on the synthesis of FO-PID controllers. *Communications in Nonlinear Science and Numerical Simulation*, 15:997–1007.

- Huang, F., Wang, L. and He, Q. 2007. An effective co-evolutionary differential evolution for constrained optimization. *Applied Mathematics and Computation*, 186(1):340–356.
- Kajita, S. and Tani, K. 1991. Study of dynamic biped locomotion on rugged terrain-theory and basic experiment. In *Fifth International Conference on Advanced Robotics (ICAR'1991)*, pages 741–746.
- Kajita, S., Kanehiro, F., Kaneko, K., Yokoi, K. and Hirukawa, H. 2001. The 3D linear inverted pendulum mode: A simple modeling for a biped walking pattern generation. In *International Conference on Intelligent Robots and Systems (IROS'2001)*, pages 239–246.
- Kajita, S., Kanehiro, F., Kaneko, K., Fujiwara, K., Harada, K., Yokoi, K. and Hirukawa, H. 2003. Biped walking pattern generation by using preview control of zero-moment point. In *IEEE International Conference on Robotics and Automation (ICRA'2003)*, Volume 2, pages 1620–1626.
- Kaynov, D., Soueres, P., Pierro, P. and Balaguer, C. 2009. *A practical decoupled stabilizer for joint-position controlled humanoid robots*. In *IEEE/RSJ International Conference on Intelligent Robots and Systems (IROS'2009)*, pages 3392–3397.
- Khatib, O., Sentis, L. and Park, J.H. 2008. A unified framework for whole-body humanoid robot control with multiple constraints and contacts. In *European Robotics Symposium 2008*, pages 303–312.
- Komura, T., Leung, H., Kudoh, S. and Kuffner, J. 2005. A feedback controller for biped humanoids that can counteract large perturbations during gait. In *2005 IEEE International Conference on Robotics and Automation (ICRA'2005)*, pages 1989–1995.
- Mistry, M., Murai, A., Yamane, K. and Hodgins, J. 2010. Sit-to-stand task on a humanoid robot from human demonstration. In *2010 10th IEEE-RAS International Conference on Humanoid Robots (Humanoids'2010)*, pages 218–223.
- Monje, C.A., Vinagre, B.M., Feliu, V. and Chen, Y.Q. 2008. Tuning and auto-tuning of fractional order controllers for industry applications. *Control Engineering Practice*, 16(7):798–812.

- Monje, C.A., Chen, Y.Q., Xue, D., Vinagre, B.M. and Feliu, V. 2010. Fractional-order Systems and Controls. Fundamentals and Applications (Advances in Industrial Control). *Springer-Verlag London*.
- Moreno, L., Garrido, S., Blanco, D. and Muñoz, M.L. 2009. Differential evolution solution to the SLAM problem. *Robotics and Autonomous Systems*, 57(4):441–450.
- Oustaloup, A., Levron, F., Nanot, F. and Mathieu, B. 2000. Frequency-band complex noninteger differentiator: characterization and synthesis. *IEEE Transaction on Circuits and Systems I: Fundamental Theory and Applications*, 47(1):25–40.
- Pan, W., Chengzhi, X. and Zhun, F. 2004. Evolutionary linear control strategies of triple inverted pendulums and simulation studies. In *Fifth World Congress on Intelligent Control and Automation (WCICA'2004)*, Volume 3, pages 2365–2368.
- Podlubny, I., Dorcak, L. and Kostial, I. 1997. On fractional derivatives, fractional order dynamic systems and $PI^{\lambda}D^{\mu}$ controllers. In *36th IEEE Conference on Decision and Control*, pages 4985–4990.
- Podlubny, I. 1999(a). Fractional Differential Equations. *Academic Press*.
- Podlubny, I. 1999(b). Fractional-order systems and $PI^{\lambda}D^{\mu}$ controllers. *IEEE Transactions on Automatic Control*, 44(1):208–214.
- Storn, R. and Price, K. 1997. Differential evolution – A simple and efficient heuristic for global optimization over continuous spaces. *Journal of Global Optimization*, 11(4):341–359.
- Tang, H., Xue, S. and Fan, C. 2008. Differential evolution strategy for structural system identification. *Computers & Structures*, 86(21-22):2004–2012.
- Tsachouridis, V.A. 1999. Robust control of a triple inverted pendulum. In *1999 IEEE International Conference on Control Applications*, Volume 2, pages 1235–1240.
- Xiaofeng, G., Hongxing, L., Guannan, D. and Haigang, G. 2009. Variable universe adaptive fuzzy control on the triple inverted pendulum and choosing contraction-expansion factor. In *International Conference on Artificial Intelligence and Computational Intelligence (AICI'2009)*, Volume 4, pages 63–67.

Xue, F., Sanderson, A.C. and Graves, R.J. 2003. Pareto-based multi-objective differential evolution. In *2003 Congress on Evolutionary Computation (CEC'2003)*, Volume 2, pages 862–869.